XVII Physics in Collision
Frascati, June 18th-19th, 1998
Conference Proceedings, pp. 000-000

RARE B DECAYS

W. T. Ford
University of Colorado, Boulder, CO 80309-0390

ABSTRACT

I describe recent discoveries of B meson decays with branching fractions of order 10^{-5} to 10^{-4}, together with their interpretation in terms of small CKM couplings and penguin loops.

1 Introduction

Charmless B decay modes are being discovered at a pace that has accelerated in the past two years. These processes may be variously interpreted in terms of small CKM couplings or higher-order loop diagrams. They consequently provide useful constraints on weak flavor mixing, non-standard model effects, and CP violation.

Recall that the third-generation b quarks have relatively small weak couplings to lighter quarks, as evidenced by the slow total decay rate, $\tau(b) \simeq 1.5$ ps. This total rate reflects primarily $b \to c$; the couplings to the first generation ($b \to u$) are even smaller, so that until a few years ago all measured B meson exclusive decay modes were to states containing charm. These direct coupling strengths are proportional to the magnitudes of elements of the CKM matrix V. Measurements of the $b \to u$ inclusive semileptonic rate, observed as a tiny tail at the edge of phase space in the lepton spectrum, give [1]

$$\left|\frac{V_{ub}}{V_{cb}}\right| \sim 0.06 - 0.10. \tag{1}$$

What we here are calling rare decay modes comprise decays involving $b \to u$, together with higher order processes. In particular, effective flavor changing neutral current transitions may be generated by penguin loops, $b \to (u,c,t)W^{\pm}$, with the virtual quark and gauge boson recombining as the virtual quark converts to s or d (see Fig. 2).

Several important measurements and searches are facilitated by the study of these decays. In general heavy quark systems are relatively amenable to theoretical treatment, in that parton level calculations need only modest corrections for quark binding. The structure of the CKM matrix is fundamental to the standard model, and determination of its third row and column (involving t and b quarks) is a problem at the current frontier. Confirmation of the unitarity of the matrix will check the completeness of the standard model with three generations, and measurement of the unitarity triangle will settle the place of CP violation in the standard model.

The penguin loops may get contributions from particles too massive to appear on-shell, giving access to top quarks and $V_{t(s,d)}$, and to Higgs, SUSY, new structure, etc. For modes that can be reached by either penguin or CKM-suppressed tree diagrams, the potential interference of amplitudes may manifest CP violation. Even for the nominally clean studies based on time evolution of CP eigenstates, a great deal of engineering involving penguin decays will be required for unambiguous interpretation of the results.

2 $B \to (\pi, \rho, \omega)\ell\nu$

The first observed exclusive final states representative of the $b \to u$ transition are $B \to (\pi, \rho, \omega)\ell\nu$, reported by the CLEO collaboration. [2] The analysis is restricted to $B\bar{B}$ pair events in which all particles but the single neutrino from this decay are detected. First, candidates are selected that contain a lepton accompanied by $\pi^{\pm}$, π^0, $\rho^{\pm}$, ρ^0, or ω. Identifying the missing four vector as $(E_\nu, \mathbf{p}_\nu)$ and cutting on $\Delta E \equiv (E_\nu + E_\ell + E_X) - E_{\text{beam}}$ one characterizes the candidate decay by its beam constrained mass $M \equiv \sqrt{E^2_{\text{beam}} - |\mathbf{p}_\nu + \mathbf{p}_\ell + \mathbf{p}_X|^2}$.

The M distributions can be combined for the different pion and vector states, since by isospin

$$\Gamma(B^0 \to \pi^- \ell^+ \nu) = 2\Gamma(B^+ \to \pi^0 \ell^+ \nu) \tag{2}$$

$$\Gamma(B^0 \to \rho^- \ell^+ \nu) = 2\Gamma(B^+ \to \rho^0 \ell^+ \nu) = 2\Gamma(B^+ \to \omega \ell^+ \nu). \tag{3}$$

The results are shown in Fig. 1. The several background sources, dominantly from the common $b \to c$ decays, are enumerated by the stacked histograms. A clear B meson peak appears in each distribution.

To turn the observations into a measurement of V_{ub}, the experimenters compare the two efficiency-corrected independent yields N_π, N_ρ, extracted from the M distribution fits, to the form-factor dependent predictions of a variety of model calculations: relativistic and non-relativistic quark models, QCD sum rules, lattice calculations (for the vector modes), and dispersion relations (for the pion modes). Allowing for the model dependence

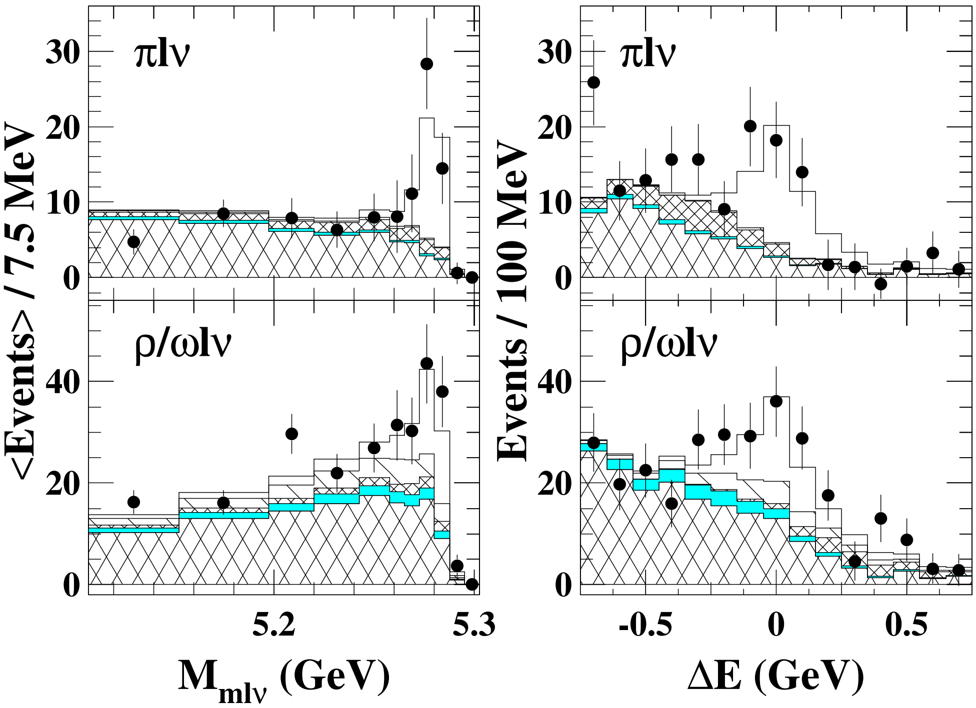

Figure 1: *Exclusive $b \to u$ decay modes reconstructed by CLEO.*

suggested by these calculations, one finds

$$| V_{ub} |= (3.3 \pm 0.2 \ {}^{+0.3}_{-0.4} \pm 0.7) \times 10^{-3}. \tag{4}$$

In combination with the results for inclusive $B \to u\ell\nu$ from ARGUS and CLEO, we find

$$| V_{ub} |= (3.2 \pm 0.7) \times 10^{-3}. \tag{5}$$

3 Radiative penguin processes

An example of an electromagnetic penguin process is the decay $B \to K^*\gamma$, which is $b \to s\gamma$ at the parton level (see Fig. 2(a)) and involves the product $V_{tb}V_{ts}$. The first observation of a penguin process was in this mode.[3] The most recent measurement from CLEO for this decay gives [4] $\mathcal{B}(B \to K^*\gamma) = (4.2 \pm 0.8 \pm 0.6) \times 10^{-5}$, including both charge states. They also search for the corresponding decays to d quarks $B \to (\rho, \omega)\gamma$. Normalizing to the $K^*\gamma$ final state we find the ratios

$$\frac{\mathcal{B}(B^- \to \rho^-\gamma)}{\mathcal{B}(B^- \to K^{*-}\gamma)} = \frac{\mathcal{B}(B^0 \to \rho^0\gamma) + \mathcal{B}(B^0 \to \omega\gamma)}{\mathcal{B}(B^0 \to K^{*0}\gamma)} = \left|\frac{V_{td}}{V_{ts}}\right| \xi\Omega, \tag{6}$$

where ξ is a correction for SU(3)-breaking and Ω is the phase space ratio. The limits from these measurements are [4]

$$\mathcal{B}(B^- \to \rho^-\gamma) \ < \ 1.1 \times 10^{-5} \tag{7}$$
$$\mathcal{B}(B^0 \to \rho^0\gamma) \ < \ 3.9 \times 10^{-5} \tag{8}$$

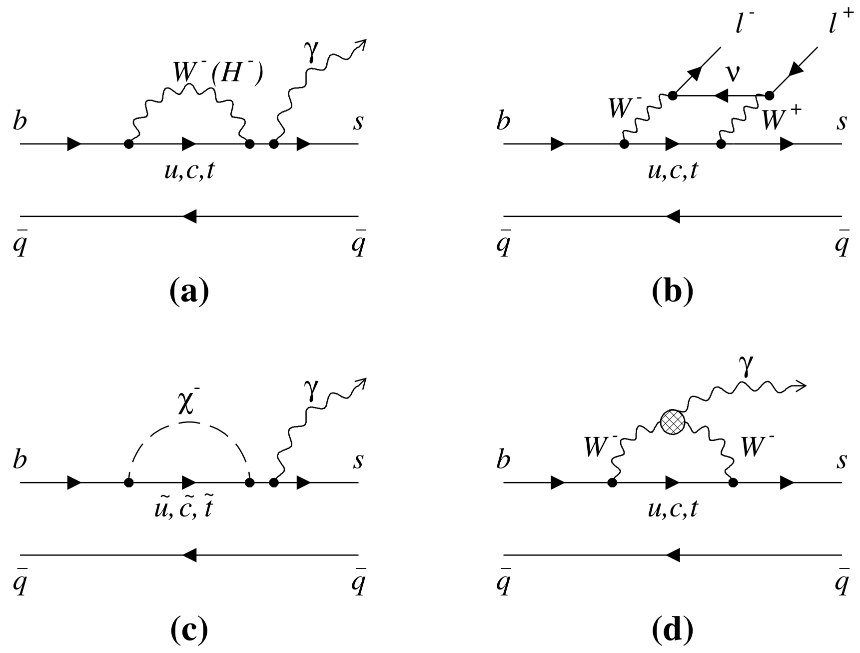

Figure 2: *Electroweak penguin Feynman diagrams: (a) radiative $b \to s$; H^- refers to a possible charged Higgs contribution. (b) One of the electroweak lepton pair radiation processes; a virtual photon or Z^0 might also convert into a lepton pair. (c) Radiative penguin mediated by a SUSY chargino. (d) The shaded circle represents a non-standard $\gamma - W^-$ coupling.*

$$\mathcal{B}(B^0 \to \omega\gamma) \quad < \quad 1.3 \times 10^{-5}, \tag{9}$$

$$\tag{10}$$

leading to

$$\left|\frac{V_{td}}{V_{ts}}\right| < 0.45 \text{ to } 0.56. \tag{11}$$

Compared with these exclusive modes, predictions of the absolute rate are more reliable for the inclusive decay $b \to s\gamma$, which has been measured by both CLEO and ALEPH. Given a measurement and the predictions of the standard model and of variants as illustrated in Fig. 2, we can place interesting limits on new physics.

On the $\Upsilon(4S)$ where B mesons are produced nearly at rest, the signature for $B \to X_s\gamma$ is a rather narrow peak in the photon spectrum just below $m_B/2$, assuming the state X_s is light compared with the B. This is illustrated in Fig. 3, which also shows the considerable background. CLEO distinguishes the backgrounds from signal by event shape measures, as suggested in Fig. 4. A large subset of the events are also matched kinematically to a list of possible exclusive states in X_s to extract the signal. The resulting distribution in the photon energy is shown in Fig. 5.

For ALEPH, running on the Z^0 resonance with negligible continuum background, the dominant background comes from $\pi^0 \to \gamma\gamma$ components of b and non-b decays of the Z^0. Fig. 6 shows the resulting photon spectrum.

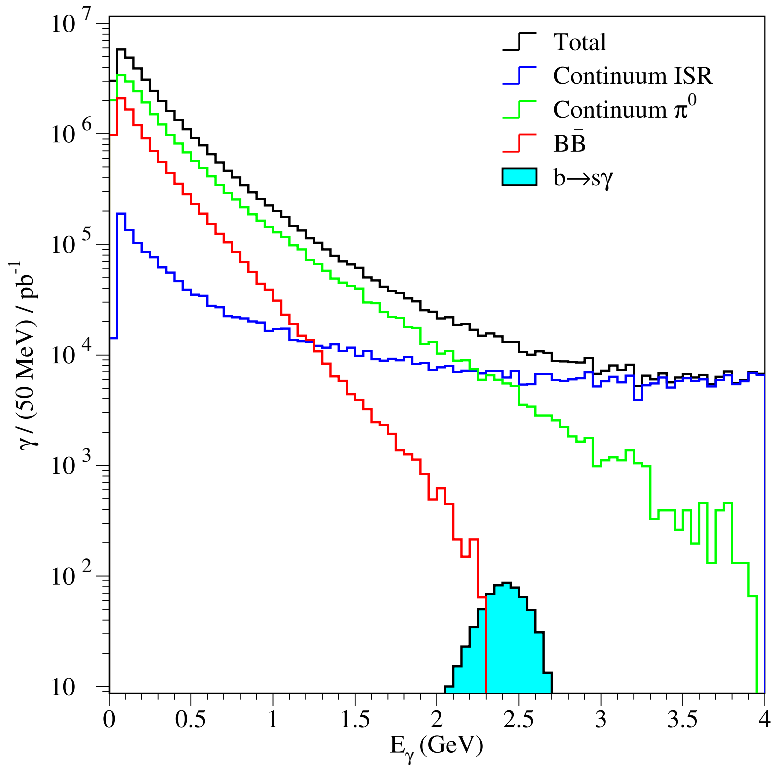

Figure 3: *Search in CLEO for $b \to s\gamma$. The background from $B \to X_c\gamma$ is the histogram cut off at 2.3 GeV. The histogram that decreases rapidly toward 4 GeV represents continuum $\pi^0 \to \gamma\gamma$ production, and the largest background component is initial state radiation in continuum events.*

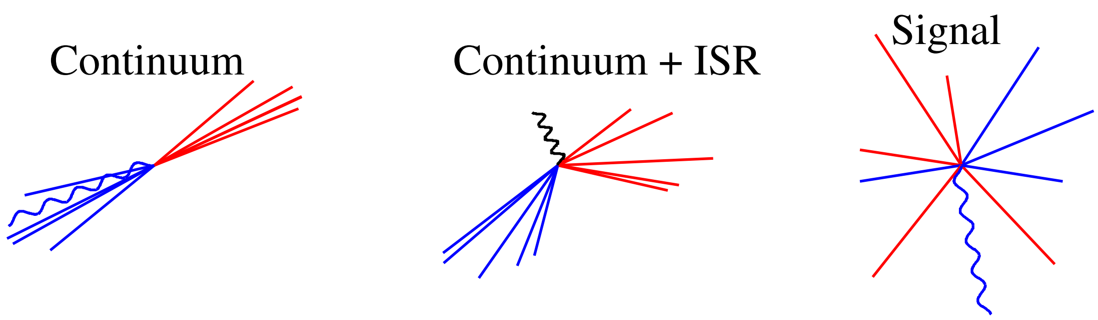

Figure 4: *Topologies of signal and background events from the $\Upsilon(4S)$.*

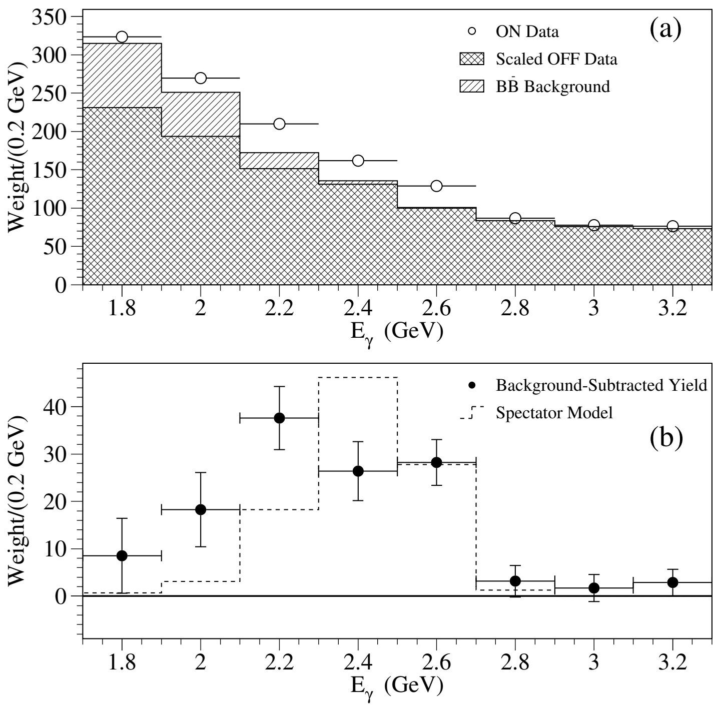

Figure 5: *CLEO E_γ spectrum (a) for $b \to s\gamma$ candidates; (b) background-subtracted spectrum.*

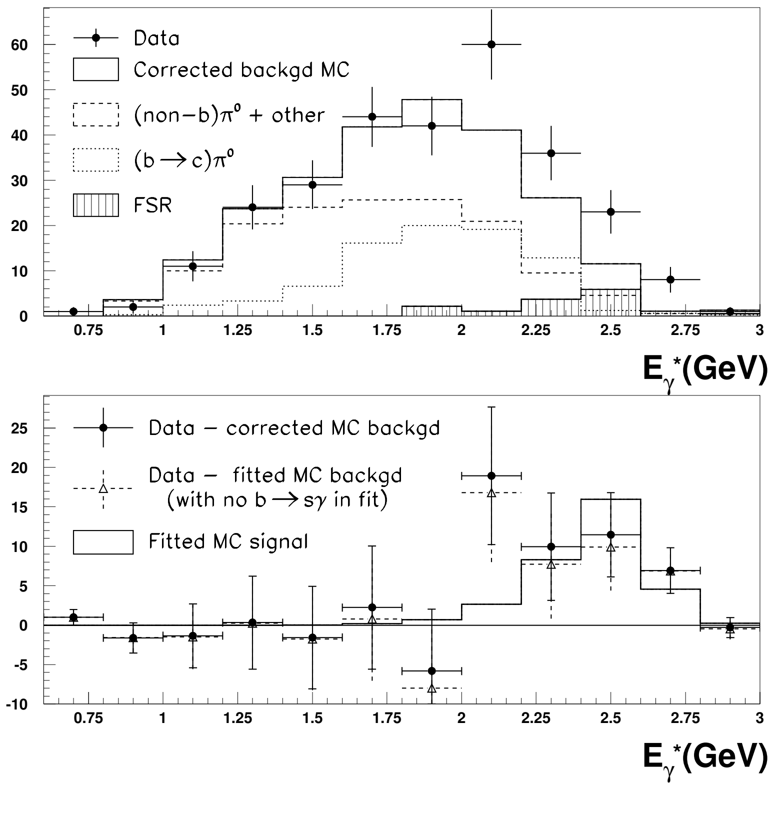

Figure 6: *ALEPH E_γ spectrum (a) for $b \to s\gamma$ candidates; (b) background-subtracted spectrum.*

CLEO's new 1998 result [6] is

$$\mathcal{B}(b \to s\gamma) = (3.15 \pm 0.35 \pm 0.32 \pm 0.26) \times 10^{-4} \tag{12}$$

(the second systematic error is for model dependence), compared with their previously published [5] $(2.32 \pm 0.57 \pm 0.35) \times 10^{-4}$. ALEPH obtains [7]

$$\mathcal{B}(b \to s\gamma) = (3.11 \pm 0.80 \pm 0.72) \times 10^{-4}. \tag{13}$$

A recent standard model calculation with 2-loop EW corrections by Czarnecki and Marciano [8] gives

$$\mathcal{B}(b \to s\gamma) = (3.28 \pm 0.30) \times 10^{-4}, \tag{14}$$

in good agreement with the measurements.

A charged Higgs as envisioned in the MSSM model would contribute through the diagram of Fig. 2(a), spoiling the consistency with observation, unless the H^+ is heavier than about 500 GeV/c^2.[9] A limit on anomalous $W - \gamma$ couplings (Fig. 2(d)) complementary to that of D0 and CDF from direct production of $W\gamma$ in $p\bar{p}$ collisions can also be extracted from these measurements, as discussed by Maderas at this conference.

4 Two body hadronic B decays

The purely hadronic final states include ones that can occur through spectator tree amplitudes analogous to the semileptonic modes, but with the virtual W materializing into a light quark pair. However, for the rare modes such diagrams are CKM suppressed, so that the penguin amplitudes come in at comparable or greater magnitude, where they are allowed. (Some modes, such as $B^+ \to K^0\pi^+$, have only penguin contributions.) Representative Feynman diagrams are shown in Fig. 7.

Where multiple amplitudes of comparable magnitude may contribute to a process we must consider interference effects. Indeed, standard model CP violation is expected in modes such as $\pi^+\pi^-$ and $\eta' K^0_s$. The former is the favored candidate for determination of the CKM unitarity angle α at the asymmetric B factories.

Theoretical approaches to the understanding of rare hadronic B decays and their relation to CP violation include phenomenological arguments based on broad symmetry principles,[10] and attempts at more complete absolute calculations.[11] The latter start with an effective Hamiltonian

$$H_{\rm eff} = -4\frac{G}{\sqrt{2}} V_{tb} V^*_{ts} \sum_{i=1}^{10} C_i(\mu) Q_i(\mu), \tag{15}$$

In which the odd (even) Wilson operators Q_i correspond to external (internal) color matching, and those labelled $i = 1, 2$ correspond to current-current amplitudes, $i = 3 - 6$ to (left- and right-handed) gluonic penguins, and $i = 7 - 10$ to electroweak penguins. The

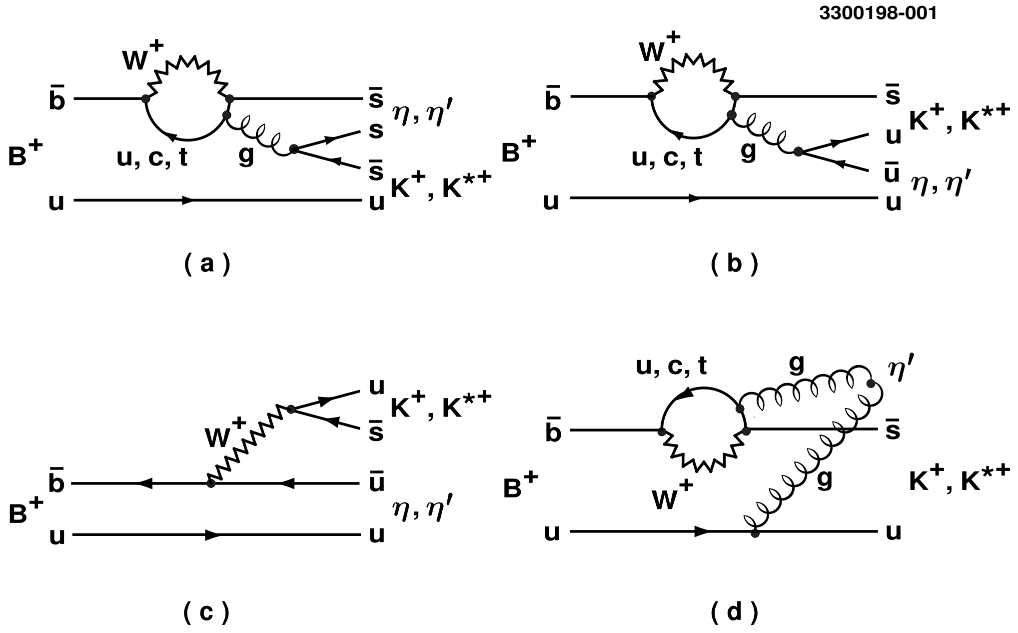

Figure 7: *Some Feynman diagrams contributing to two-body hadronic decays.*

renormalization group evolution $\mu = m_W \to m_B$ mixes the operators while preserving the scale independence of $\sum C_i(\mu)Q_i(\mu)$, up to neglected terms in the perturbation series.

One then seeks an approximate factored form of the matrix element

$$\langle m_1 m_2 \mid H_2 \mid B\rangle = \langle m_1 \mid J^\mu \mid B\rangle\langle m_2 \mid J_\mu \mid 0\rangle. \tag{16}$$

Some of the terms require a Fierz transformation to achieve this factorization, which scrambles color indices and generates a color octet-octet term. Since this term is unmeasurable, one ignores it and replaces factors $1/N_c$, where N_c is the number of colors, by a parameter ξ to be fit to data.

Other uncertainties in the calculations include dependence of $\langle m_2 \mid J_\mu \mid 0\rangle$ on the decay constant f_{m_2}, dependence of $\langle m_1 \mid J^\mu \mid B\rangle$ on form factors $F_{B\to m_1}$ and its counterparts for pseudoscalar or vector m_1, quark masses, and the average 4-momentum of virtual gluons and photons in loops.

On the experimental side, ALEPH [12)] has reported a candidate event for $B^0 \to K^+\pi^-$, with a clear separation between the primary and B decay vertices. DELPHI [13)] has reconstructed candidates for final states with K, π, ρ, and a_1. The mass distribution shows an excess of a few events at the B mass.

CLEO has conducted extensive searches based on about six million produced B mesons from the $\Upsilon(4S)$. Here the B mesons are nearly at rest in the laboratory ($p_B \simeq 300$ MeV/c). The B meson mass is $m_B \simeq 5.3$ GeV/c^2, so for two-body decays the daughters are nearly back-to-back with energy $\simeq 2.6$ GeV. Energy and momentum conservation are imposed by requirements that $\Delta E \equiv \sum E_i - E_{\rm beam}$ be zero within resolution, and that $M \equiv \sqrt{E_{\rm beam}^2 - |\mathbf{p}_i|^2}$ be similarly compatible with m_B. ($E_{\rm beam}$ is much better measured than $\sum E_i$ in CLEO.)

Compared with the expected signals, backgrounds from $b \to c$ are characterized by heavier daughters, hence lower recoil energies. Continuum background (e.g. two $x = .5$ particles in opposite jets from $e^+e^- \to q\bar{q}$) are distinguished by event shape, and by the property that the B decay axis is uncorrelated with the jet axis, while background is strongly correlated. Continuum background is studied in data samples recorded with $E_{\rm cm} < B\bar{B}$ threshold.

4.1 $B \to (K,\pi)\pi$

CLEO's search for decays to kaon and/or pion spans all of the possible charge states. They report positive observations [14] of $B^0 \to K^+\pi^-$, $B^+ \to h^+\pi^0$ (where h^+ is a charged kaon or pion), and $B^+ \to K^0\pi^+$. Distributions of these candidates in M and ΔE are shown in Fig. 8. The overlaid curves are projections from a likelihood fit to the data of a function of several variables, including event shape measures and particle identification.

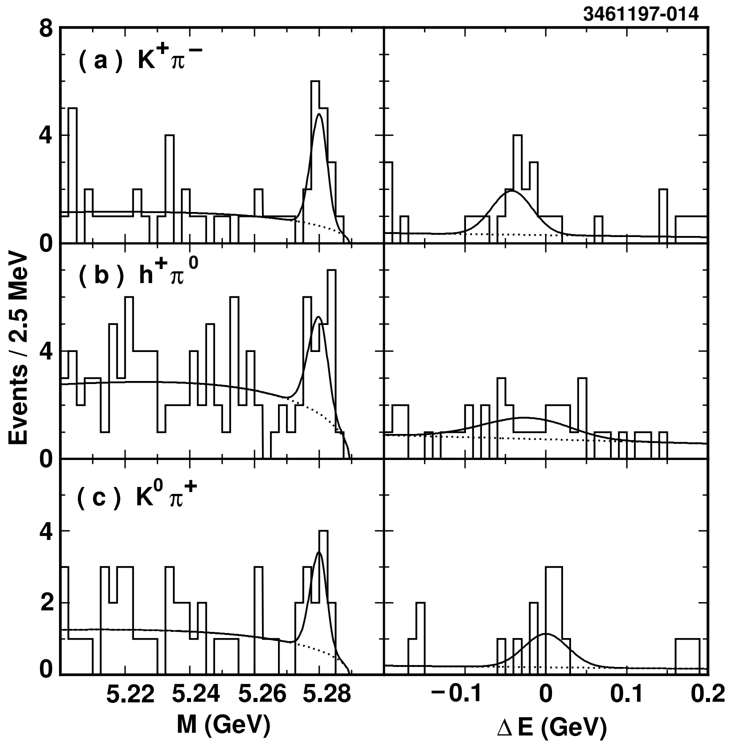

Figure 8: *B candidate beam-constained effective mass (left) and energy residual (right), for K,π modes seen by CLEO. In the calculation of ΔE the pion mass was assumed for the K^+ in (a) and the h^+ in (b), leading to a downward shift of* $\simeq 40$ MeV.

In these data charged kaons are distinguished from pions by kinematics (the mass assumed in the calculation of ΔE) and by dE/dx in the drift chamber. Some ambiguity persists, which is resolved statistically for the sample. The likelihood function for the modes subject to this ambiguity are shown in Fig. 9, from which one can judge the significance of either hypothesis.

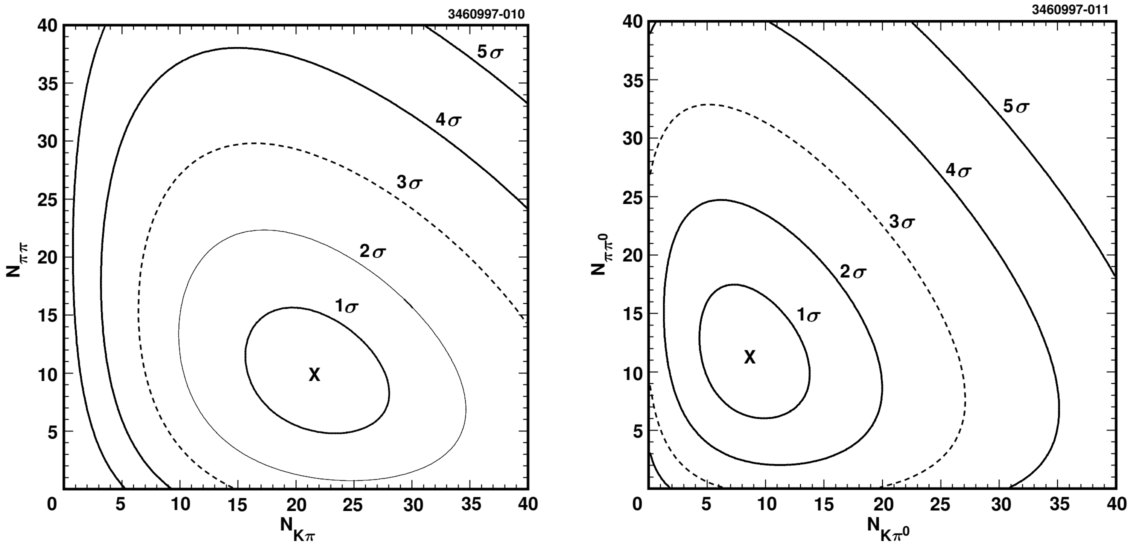

Figure 9: *Likelihood contours from CLEO data for $B \to h\pi$ (left), and $B \to h\pi^0$ (right).*

Table 1: *Results for some two body hadronic modes (CLEO). Where two systematic errors are quoted, the first is for the fitted yield, the second for the efficiency estimate (which does not affect the significance).*

Decay mode	Branching fraction $\times 10^5$	Comparison	Comment
$B^0 \to K^+\pi^-$	$1.5^{+0.5}_{-0.4} \pm 0.1 \pm 0.1$	~ 1.4 to 2.1	$H_{\rm eff}$, factorization [17]
$B^0 \to \pi^+\pi^-$	< 1.5	1.2 ± 0.4	$B \to \pi\ell\nu$, factorization
$B^+ \to h^+\pi^0$	$1.6^{+0.6}_{-0.5} \pm 0.3 \pm 0.2$		
$B^+ \to K^+\pi^0$	< 1.6		
$B^+ \to \pi^+\pi^0$	< 2.0	0.6 ± 0.2	$B \to \pi\ell\nu$, factorization
$B^+ \to K^0\pi^+$	$2.3^{+1.1}_{-1.0} \pm 0.3 \pm 0.2$	$< \frac{\mathcal{B}(B^0\to K^+\pi^-)}{\sin^2\gamma}$	$\gamma_{\rm CKM}$ bound [18]
$B^+ \to \eta' K^+$	$6.5^{+1.5}_{-1.4} \pm 0.9$		
$B^0 \to \eta' K^0$	$4.7^{+2.7}_{-2.0} \pm 0.9$		
$B^+ \to \omega K^+$	$1.5^{+0.7}_{-0.6} \pm 0.2$		
$B^0 \to \omega h^+$	$2.5^{+0.8}_{-0.7} \pm 0.3$		
$B \to \phi K^*$	$1.1^{+0.6}_{-0.5} \pm 0.2$		

Fleischer and Mannel [18] have proposed a constraint on $\gamma_{\rm CKM}$ that can in principle be obtained from these measurements. They note that $B^+ \to K^0\pi^+$ is a pure penguin process. Defining the modulus and phase (r, ϕ) of the tree to penguin ratio and the measurable branching fraction ratio R they find:

$$
\begin{aligned}
r &\equiv (\text{tree})/(\text{penguin}); \quad \delta \equiv \phi_{(\mathbf{tree})} - \phi_{(\mathbf{penguin})} && (17)\\
R &\equiv \mathcal{B}\left(B^0 \to K^+\pi^-\right)/\mathcal{B}\left(B^+ \to K^0\pi^+\right) && (18)\\
R &= 1 - 2r\cos\delta\cos\gamma + r^2 && (19)\\
\sin^2\gamma &< R = 0.65 \pm 0.38, && (20)
\end{aligned}
$$

where we have evaluated R from the data in Table 1. The present measurement is not quite precise enough for a useful limit. The literature contains several contributions from these authors and others expanding on complications for this interpretation from final state interactions, etc.

4.2 $B \to \eta' K$

In a comprehensive search for decays to η and η', CLEO found significant signals in both charge modes of $B \to \eta' K$. The mass distributions and likelihood functions are shown in Fig. 10, and results for the branching fractions appear in Table 1. The branching fraction for the charged mode is somewhat large compared with the factorization prediction, which is dependent on the parameter ξ, and constrains ξ to a fairly small value. Because the η' is an $I = 0$ meson with large flavor-SU(3) singlet admixture, it may be formed through a pure (two or more) gluon intermediate state ("hairpin", Fig. 7 (d)). Thus the large rate could be suggesting the importance of the QCD gluon anomaly or other flavor singlet processes in constructive interference with the penguins. Other possibilities include charm enhancement in the penguins or in the η' wave function.

4.3 $B \to \omega K$, $B \to \phi K^*$

In their search for vector meson modes CLEO have found a significant signal for $B^+ \to \omega K^+$. The likelihood function and mass distribution are shown in Fig. 11. The ωh^+ branching fraction, listed along with ωK^+ in Table 1, is large enough to leave room possibly for $\omega\pi^+$ as well. The individual modes with ϕ mesons do not show significant signals, but taken collectively they offer a hint for $B \to \phi K^*$.

The factorization calculation for $B^+ \to \omega h^+$ is quite sensitive to the parameter ξ, and is most compatible with the data for large values of ξ (somewhat inconsistent with ξ from $B \to \eta' K$). As more measurements of these small branching fractions become available the ability of these models to accommodate all of the data will doubtless be further challenged.

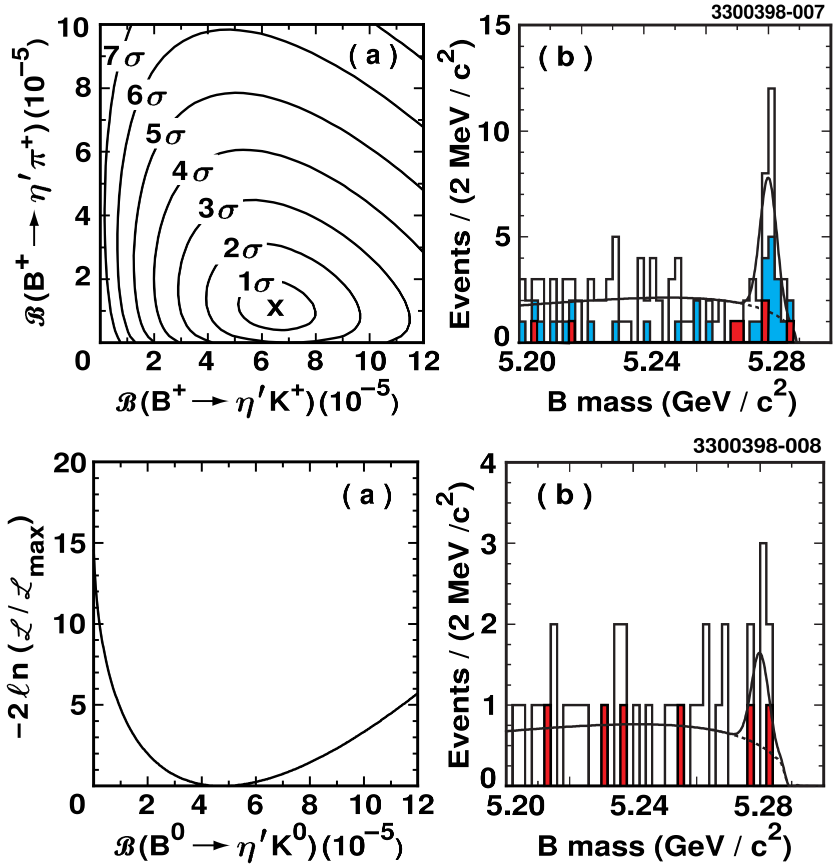

Figure 10: *Likelihood function (a) and B candidate beam-constrained effective mass distribution (b) for $B^+ \to \eta' h^+$ (above) and $B^0 \to \eta' K^0$ (below).*

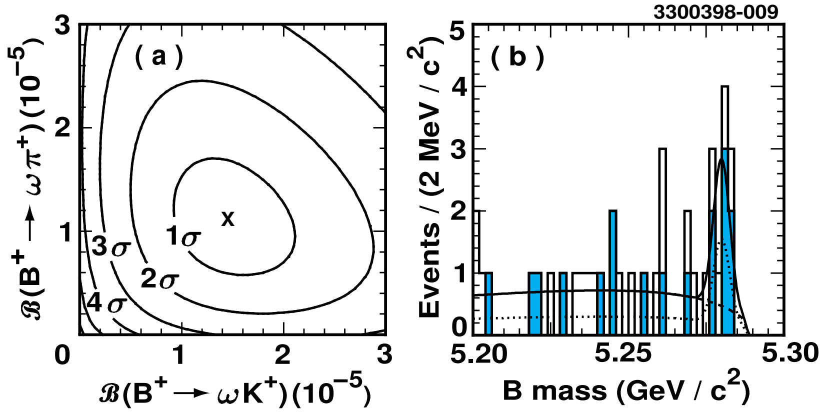

Figure 11: *Likelihood function (a) and B candidate beam-constrained effective mass distribution (b) for $B^+ \to \omega h^+$.*

4.4 Limits on other hadronic modes

Considering all combinations of the S-wave pseudoscalar and vector meson nonet members there are some 81 two body decays, 76 if we restrict ourselves to those with spectator interpretation. Figures 12 and 13 show CLEO's measurements and limits for a large number of searches, alongside the theoretical estimates.

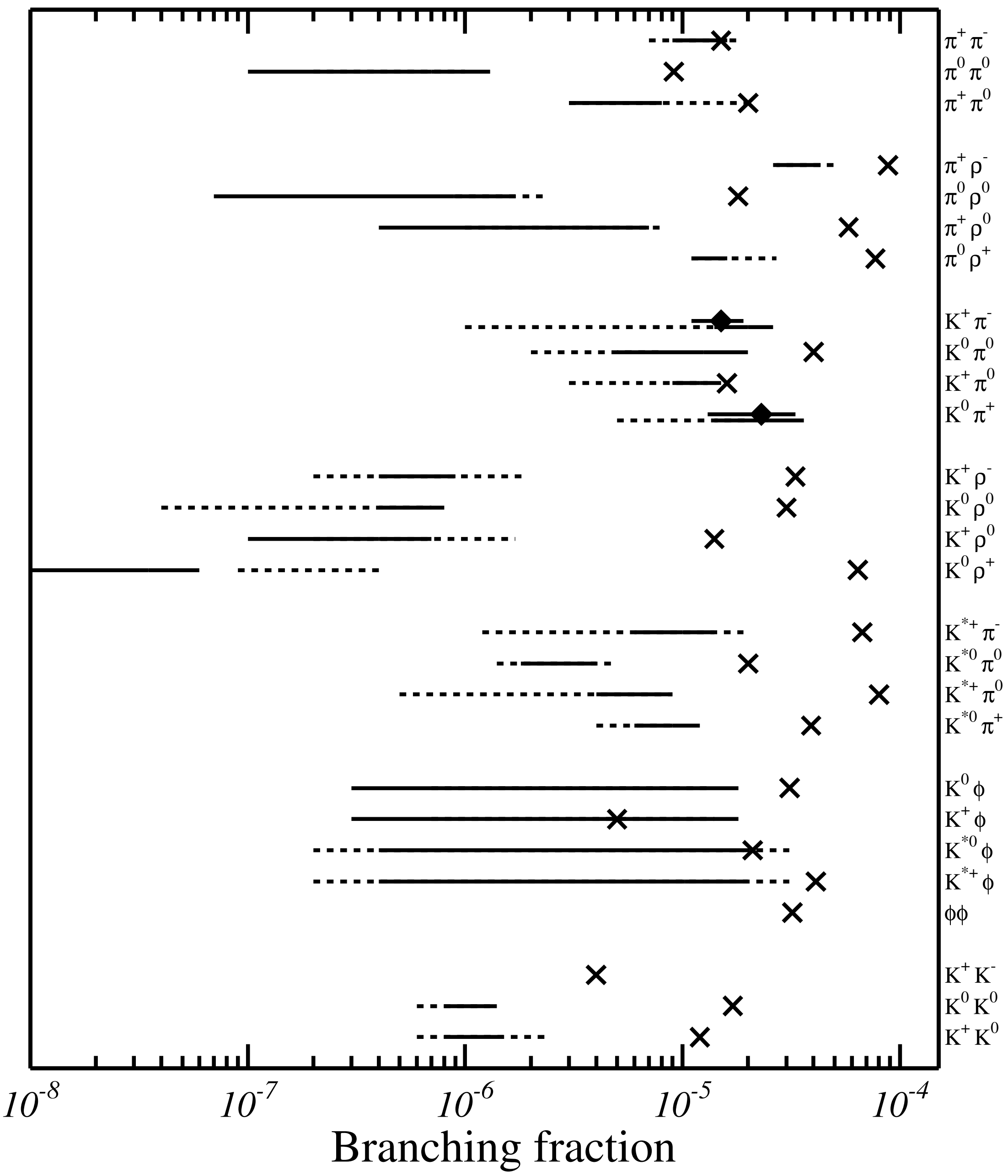

Figure 12: *Summary of modes with K, π from CLEO.*

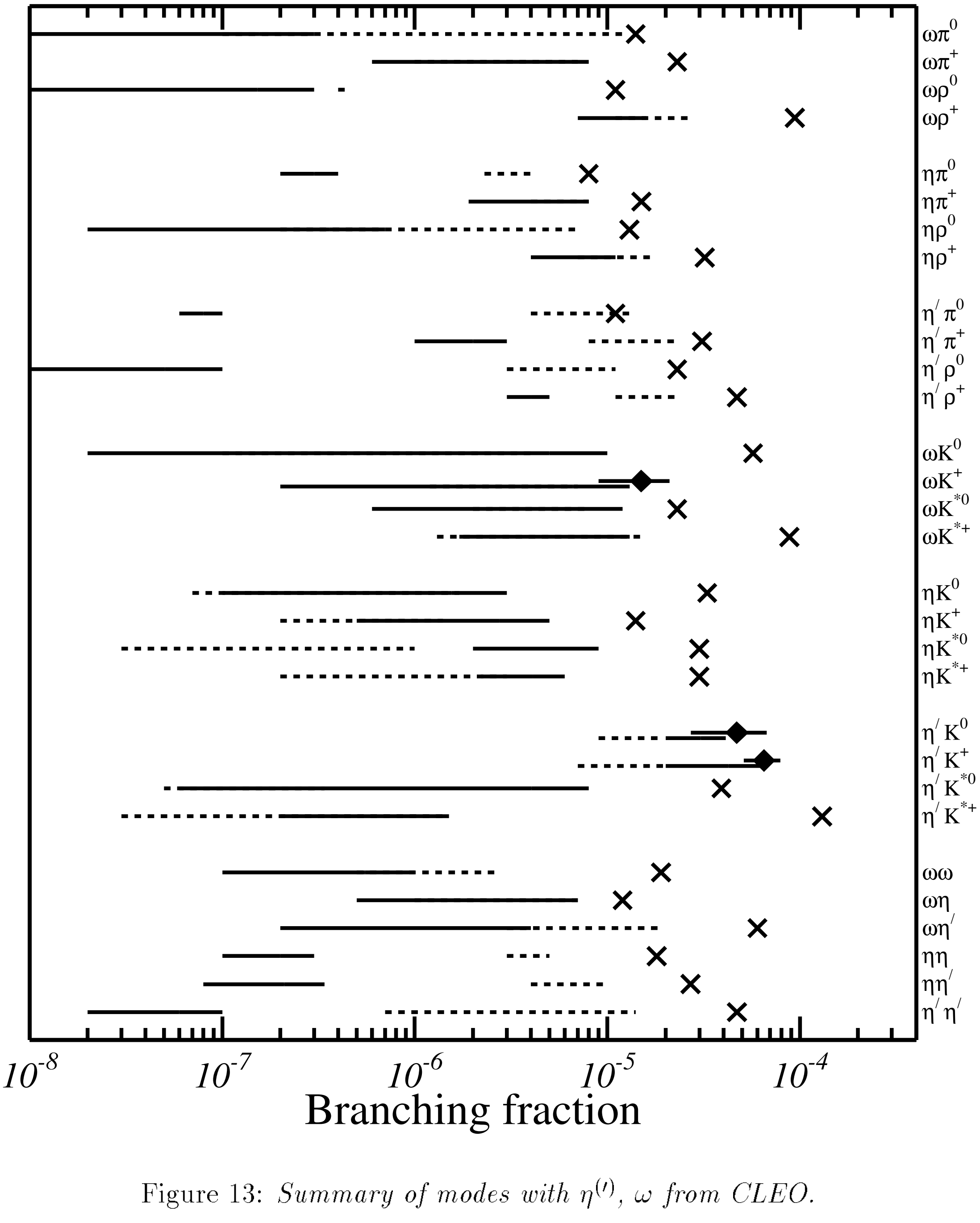

Figure 13: *Summary of modes with $\eta^{(\prime)}$, ω from CLEO.*

5 Inclusive B decays to η'

Following an approach similar to that used for $b \to s\gamma$, CLEO has searched for inclusive charmless B decays with an η or η', as a possible signature for $b \to sg$. They first select a high momentum ($2.0-2.7$ GeV/c) $\eta' \to \pi\pi\eta$, $\eta \to \gamma\gamma$ candidate, accompanied by a kaon in combination with multiple pions with kinematics consistent with $B \to \eta^{(\prime)} X_s$. The η' candidate mass distribution is shown in Fig. 14, indicating the presence of inclusive η' events.

The potential backgrounds in this sample include the tail of $b \to c$, especially color-suppressed D modes, and feed across from nonstrange rare B decays. Assuming the observed events can be interpreted as $b \to sg^*$, they find [19]

$$\mathcal{B}\,(B \to \eta' X_s) \;=\; \left(6.2 \pm 1.6\ (\mathrm{stat}) \pm 1.3\ (\mathrm{sys})^{+0.0}_{-1.5}\ (\mathrm{bkgd})\right) \times 10^{-4}, \qquad (21)$$

$$(\mathcal{B}\,(B \to \eta X_s) \;<\; 4.4 \times 10^{-4}) \qquad (22)$$

The η' branching fraction exceeds most calculations. As with the exclusive $B \to \eta' K$, possible interpretations include large $c\bar{c}$ content of η', enhanced charm in the penguin loop, the QCD anomaly, or constructive interference of several processes.[20]

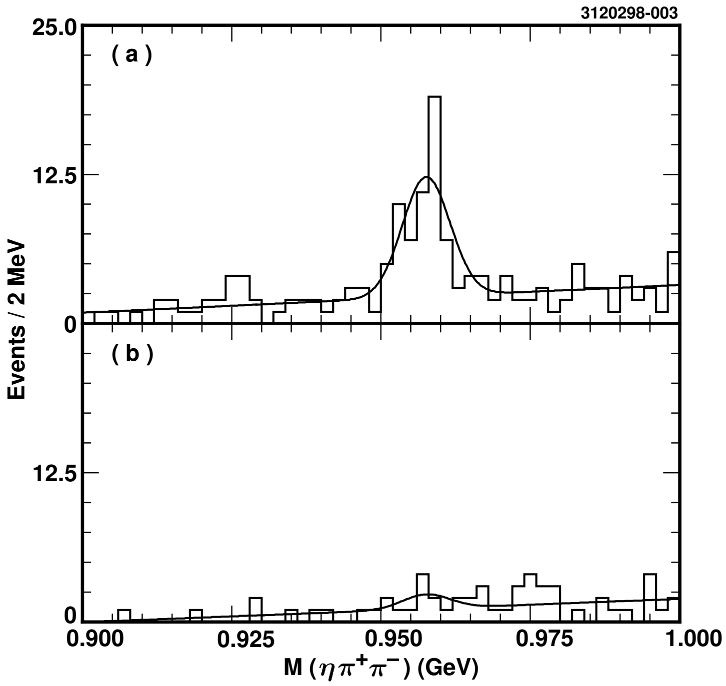

Figure 14: *$\pi\pi\eta$ mass distribution for (a) $B \to \eta' X_s$ candidates, and (b) below-resonance data.*

6 Conclusions

Experiments have begun to explore the $\mathcal{O}(10^{-5})$ decade of branching fractions in B decays. About ten exclusive modes have been observed so far: semileptonic $(\pi, \rho)\ell\nu$, radiative penguin $K^*\gamma$, and the hadronic two-body $K\pi$ (two charge states), $K\eta'$ (two charge states), $K^+\omega$, and $K^*\phi$ (semi-inclusive). Inclusive modes that have been seen are $X_u\ell\nu$, $X_s\gamma$, and $X_{(s)}\eta'$.

These measurements have stimulated much theoretical interest and effort. Note that we still haven't positively observed $B\to\pi^+\pi^-$. More data in are hand, with much more in prospect over the next few years from B factories.

7 Acknowledgements

I have benefitted from discussions with Jean Roy, Jim Smith, Lawrence Gibbons, Roy Briere, Ritchie Patterson, and many others among my CLEO collaborators. I drew on earlier presentations by Briere and Steve Glenn, and Ref. 9. I would like to thank the organizers of the conference a most productive exchange in a delightful setting. This work was supported in part by the Department of Energy under Grant DE-FG03-95ER40894.

References

1. CLEO Collaboration (J. Bartelt et al.) *Phys. Rev. Lett.* **71**, 4111 (1993).

2. CLEO Collaboration (J. P. Alexander et al.) *Phys. Rev. Lett.* **77**, 5000 (1996).

3. CLEO Collaboration (R. Ammar et al.), *Phys. Rev. Lett.* **71**, 674 (1993).

4. CLEO Collaboration (R. Ammar et al.), Paper contributed to the *International Conference on High Energy Physics*, CLEO CONF 96-05, ICHEP96 PA05-093 (1996).

5. CLEO Collaboration (M. S. Alam et al.) *Phys. Rev. Lett.* **74**, 2885 (1995).

6. CLEO Collaboration (S. Glenn et al.) CLEO CONF 98-17, ICHEP98 1011 (1998).

7. ALEPH Collaboration (R. Barate et al.) *Phys. Lett.* B **429**, 169 (1998).

8. Andrzej Czarnecki and William J. Marciano, *Phys. Rev. Lett.* **80**, 277 (1998).

9. Karen Lingel, Tomasz Skwarnicki, and J. G. Smith, COLO–HEP–403, SLAC-PUB-7796, HEPSY 98-1, to appear in *Annual Reviews of Nuclear and Particle Science* (1998).

10. Michael Gronau and Jonathan L. Rosner, Phys. Rev. D**53**,2516 (1996); A. S. Dighe, Phys. Rev. D **54**, 2067 (1996); M. Gronau and J. L. Rosner, Phys. Rev. Lett. **76**, 1200 (1996); G. Kramer, W. F. Palmer, and H. Simma, Zeit. Phys. C **66** 429 (1995); A. S. Dighe, M. Gronau, and J. L. Rosner, Phys. Rev. Lett. **79**, 4333 (1997); H. J. Lipkin, Phys. Lett. B **254**, 247 (1991); D. London and A. Soni, Phys. Lett. B **407**, 61 (1997).

11. M. Bauer, B. Stech, and M. Wirbel, Z. Phys. C**43**, 103 (1987); L.-L. Chau *et al.*, Phys. Rev. D **43**, 2176 (1991); A. Deandrea *et al.*, Phys. Lett. B **318**, 549 (1993); **320**, 170 (1994); N. G. Deshpande, B. Dutta, and S. Oh, Report No. OITS-641 (1997); Ref. 17.

12. ALEPH Collaboration (D. Buskulic et al.) *Phys. Lett.* B **384**, 471 (1996).

13. DELPHI Collaboration (W. Adam et al.) *Z. Phys.* C **72**, 207 (1996).

14. CLEO Collaboration (R. Godang et al.) *Phys. Rev. Lett.* **80**, 3456 (1998).

15. CLEO Collaboration (B. Behrens et al.) *Phys. Rev. Lett.* **80**, 3710 (1998).

16. CLEO Collaboration (T. Bergfeld et al.) *Phys. Rev. Lett.* **81**, 272 (1998).

17. A. Ali, G. Kramer, and Cai-Dian Lü, DESY 98-041 (1998).

18. R. Fleischer and T. Mannel, *Phys. Rev.* D **57**, 2752 (1998).

19. CLEO Collaboration (T. E. Browder et al.) Cornell preprint CLNS 98/1544 (1998).

20. David Atwood and Amarjit Soni, Phys. Lett. B **405**, 150 (1997).